

# Weakly-Supervised 3D Visual Grounding based on Visual Linguistic Alignment\*

Xiaoxu Xu\*, Yitian Yuan\*, Qiudan Zhang, Wenhui Wu, Zequn Jie, Lin Ma, Xu Wang

## Abstract

Learning to ground natural language queries to target objects or regions in 3D point clouds is quite essential for 3D scene understanding. Nevertheless, existing 3D visual grounding approaches require a substantial number of bounding box annotations for text queries, which is time-consuming and labor-intensive to obtain. In this paper, we propose **3D-VLA**, a weakly supervised approach for 3D visual grounding based on **Visual Linguistic Alignment**. Our 3D-VLA exploits the superior ability of current large-scale vision-language models (VLMs) on aligning the semantics between texts and 2D images, as well as the naturally existing correspondences between 2D images and 3D point clouds, and thus implicitly constructs correspondences between texts and 3D point clouds with no need for fine-grained box annotations in the training procedure. During the inference stage, the learned text-3D correspondence will help us ground the text queries to the 3D target objects even without 2D images. To the best of our knowledge, this is the first work to investigate 3D visual grounding in a weakly supervised manner by involving large scale vision-language models, and extensive experiments on ReferIt3D and ScanRefer datasets demonstrate that our 3D-VLA achieves comparable and even superior results over the fully supervised methods.

## Introduction

3D visual grounding (3D-VG), which aims to precisely identify target objects in a 3D scene with the corresponding natural language queries, has gained considerable attention over the past few years (Achlioptas et al. 2020; Chen, Chang, and Nießner 2020; Yuan et al. 2021; Chen et al. 2022a; Yang et al. 2021; Chen et al. 2022b). Previous works (He et al. 2021; Zhao et al. 2021; Huang et al. 2021; Feng et al. 2021) mainly explore fully supervised solutions for 3D-VG, as shown in Fig.1 (a), the 3D bounding box for the text query is provided during the training procedure, which helps the model to establish the explicit alignment between the two modalities. However, annotating dense 3D boxes in point clouds is labor-intensive and expensive, therefore it hinders large scale datasets collection, and further influences the model capability of 3D-VG.

To solve the above challenge, a natural way is to investigate 3D-VG in a weakly supervised manner that does not

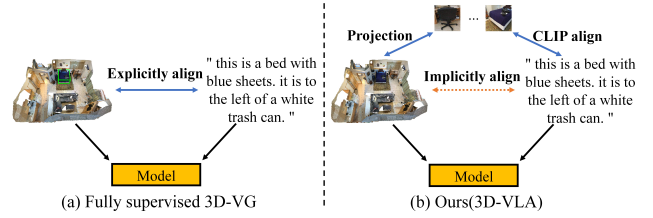


Figure 1: The comparison of fully supervised and our proposed weakly supervised 3D visual grounding. Our method leverages natural 3D-2D correspondence from geometric camera calibration and 2D-text correspondence from large-scale vision-language models to implicitly align texts and 3D point clouds.

need dense and fine-grained 3D box annotations. Such idea has been explored in 2D visual grounding (2D-VG), which mainly focus on establishing semantic (Li et al. 2022b, 2023) correspondences between 2D image and text descriptions (Datta et al. 2019; Gupta et al. 2020; Li et al. 2022a; Liu et al. 2021). However, different from 2D images, 3D point clouds inherently provide essential geometric information and surface context with a higher level of complexity and a larger spatial scale, and bring new challenges to effectively learning the matching relationships between 3D point clouds and texts. It may be difficult to explicitly correlate texts and 3D point clouds, but we can notice that, the correspondences between 3D point clouds and 2D images can be easily obtained by geometric camera calibration with intrinsic and extrinsic parameters. At the same time, we can also note that the current large-scale vision-language pre-trained models (VLMs) such as CLIP (Radford et al. 2021), ViLT (Kim, Son, and Kim 2021), VLMO (Bao et al. 2022) have been greatly developed. Using massive text-image pairs for model training, VLMs are able to establish precise semantic matching relationships between natural languages and 2D images, and have achieved good results in various downstream tasks such as image classification, VQA, and image captioning. So, as shown in Fig.1 (b), why don't we take 2D images as a bridge, leveraging the correspondences between point clouds and images, images and natural languages, to implicitly build matching relationships between point clouds and natural languages?

To this end, we present a novel weakly supervised method

\* The paper is under consideration at Computer Vision and Image Understanding

**3D-VLA**, which explores the **3D** visual grounding based on the **Visual Linguistic Alignment** while without the need of 3D bounding box annotations. Specifically, as shown in Fig. 2, in the training stage, our 3D-VLA possesses a text module, a 2D module, and a 3D module. We first extract 3D proposal candidates from the point cloud scene and project these proposals to 2D image regions through geometric camera calibration, and then we utilize a frozen CLIP model to get the embeddings of the text query and 2D image regions with its text encoder and image encoder, respectively. The correspondences between the text query and 2D image regions can thus be measured through their CLIP embeddings. We leverage contrastive learning to optimize the 3D encoder in the 3D module by making the learned 3D embeddings comparable to the text and 2D CLIP embeddings. If a 2D image region and a 3D proposal are matched in pairs, their embeddings should be pulled closer, otherwise they should be pushed further apart.

Ideally, if the 3D embedding of a proposal candidate is learned well enough, it can be directly compared with the text query embedding by the similarity measurement to judge whether it is the target proposal. However, we also find that only relying on the implicit contrastive learning is not reliable since the pretrained data of VLMs are general and do not have specialized knowledge to the indoor point cloud scene. We propose to alleviate this problem by introducing multi-modal adaption through task-aware classification. As shown in Fig. 2, we first add three adapters to transfer the text, 2D and 3D embeddings to another embedding space, and then the 2D and 3D classification are realized by comparing the adapted region/proposal embeddings to the text embeddings of the category labels in the dataset. For the query, we directly apply a text classifier on its adapted query embedding, thus obtaining its distribution on the category labels. By introducing the task-aware classification signal of 3D-VG in the indoor point cloud scene, we can further align the semantic relationships among texts, 2D images and 3D point clouds specialized for 3D visual grounding.

In the inference stage, as shown in Fig. 3, we can completely ignore the 2D image module and directly compare the learned 3D point cloud embeddings and text embeddings to determine the target proposal. At the same time, we can also use the classification results of text and 3D objects to filter out some confusing and unreliable predictions. In summary, the main contributions of this paper are as follows:

- We propose a weakly supervised method 3D-VLA for 3D-VG, which takes 2D images as a bridge, and leverages natural 3D-2D correspondence from geometric camera calibration and 2D-text correspondence from large-scale vision-language models to implicitly establish the semantic relationships between texts and 3D point clouds.
- Our 3D-VLA utilizes contrastive learning to get 3D proposal embeddings that can basically align with the 2D and text embeddings from VLMs, and the introduced multi-modal adaption through task-aware classification also guides the learned embeddings to better support 3D visual grounding.

- Extensive experiments are conducted on two public datasets, and the experimental results demonstrate that our proposed 3D-VLA can achieve comparable and even superior results over the fully supervised methods. Our 3D-VLA and its results provide valuable insights to improve further research of weakly supervised 3D visual grounding.

## Related Work

### Weakly Supervised Visual Grounding on Images

In contrast to the traditional supervised 2D visual grounding, the weakly supervised setting focuses on learning the fine-grained correspondence between regions and phrases without relying on target bounding box annotations. In recent studies, a general approach for weakly supervised visual grounding (Rohrbach et al. 2016; Chen, Gao, and Nevatia 2018; Liu et al. 2019; Wang et al. 2020; Dou and Peng 2021; Qu, Tuytelaars, and Moens 2023) involves a hypothesis-and-matching strategy. Initially, a set of region proposals is generated from an image using an external object detector (Salvador et al. 2016). Subsequently, the model performs a matching process between query phrases and these generated regions to establish the relevant connections.

### 3D Visual Grounding

The objective of 3D visual grounding is to precisely locate a targeted object in a 3D scene based on a given query that describes the target. The primary benchmark datasets for 3D visual grounding include ReferIt3D (Achlioptas et al. 2020) and ScanRefer (Chen, Chang, and Nießner 2020), both of which are based on the ScanNet (Dai et al. 2017). Previously, most approaches (Huang et al. 2022; Bakr, Alsaedy, and Elhoseiny 2022) adopt a two-stage pipeline. In the first stage, they employ a 3D object detector to generate object proposals. In the second stage, they search for the target proposal that best matches the given query. To address the issue of imprecise object proposals generated in the first stage, some one-stage pipeline (Jain et al. 2022; Luo et al. 2022; Wu et al. 2023) are introduced. Those approach aim to improve the accuracy of object proposals, thus enhancing the overall performance of 3D visual grounding.

However, those methods mentioned above are all fully supervised, which need much expensive bounding box annotations. To overcome this shortcoming, we propose the first 3D weakly supervised visual grounding method.

## Method

In this section, we will first demonstrate our 3D-VLA training procedure by visual linguistic alignment. Then, we will describe the inference procedure of 3D-VLA with category-oriented proposal filtering.

### 3D-VLA Training by Visual Linguistic Alignment

As shown in Fig. 2, the inputs of 3D-VLA comprises a 3D point cloud scene and a text query  $Q$ . The point cloud scene  $S \in \mathbb{R}^{N \times 6}$ , which indicates there are  $N$  points in the scene, and each point is represented with six dimensions RGBXYZ. The 3D object proposals for the scene are readily

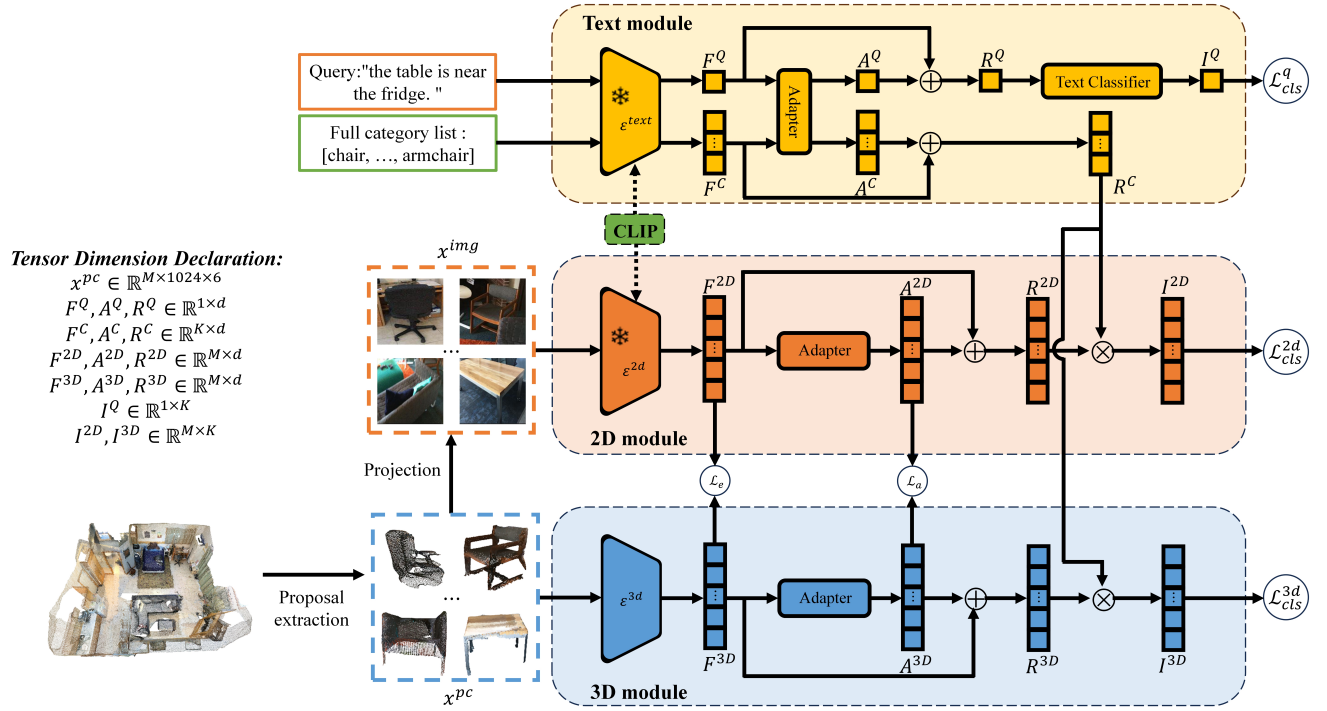


Figure 2: The training procedure of our proposed 3D-VLA. We first extract 3D proposal candidates  $x^{pc}$  from the point cloud scene and use geometric camera calibration to project them to 2D image regions  $x^{img}$ . Then we leverage the text encoder  $\epsilon^{text}$  of CLIP to get embedding of the text query  $F^Q$  and embedding of the category labels  $F^C$ , and leverage the 2D image encoder  $\epsilon^{2d}$  of CLIP to get embeddings of 2D image regions  $F^{2D}$ . It is important to note that we freeze the whole CLIP model during training. Meanwhile, we use 3D encoder  $\epsilon^{3d}$  to encode the 3D proposal candidates and get their 3D embeddings  $F^{3D}$ . Three adapters are further introduced to transfer the  $F^C$ ,  $F^Q$ ,  $F^{2D}$ ,  $F^{3D}$  to a new embedding space for coarse-grained classification in the indoor scene domain. We use contrastive learning to align the 2D CLIP embedding  $F^{2D}$  and the encoded 3D embedding  $F^{3D}$ , and also align their corresponding adapted embeddings  $A^{2D}$  and  $A^{3D}$ . The classification loss  $\mathcal{L}_{cls}^q$ ,  $\mathcal{L}_{cls}^{2d}$ ,  $\mathcal{L}_{cls}^{3d}$  and the contrastive loss  $\mathcal{L}_e$  and  $\mathcal{L}_a$  will be integrated to train the overall model.

available, either generated from the off-the-shelf 3D object detector (Jiang et al. 2020). These proposals will serve as the initial candidate proposals for 3D visual grounding. In each dataset, the category labels are also provided for the 3D objects, we will also encode all of these category labels to get their embeddings, so as to support the coarse-grained classification task to help the model learning.

**3D Encoder.** For the 3D proposal candidates, we first sample 1024 points for each of them, and then leverage PointNet++ (Qi et al. 2017) to do the initial feature encoding, followed by a standard transformer (Vaswani et al. 2017) to extract higher-level 3D semantic embeddings  $F^{3D} = \{F_1^{3D}, \dots, F_M^{3D}\}$ , where  $M$  is the total number of 3D proposal candidates. The above procedures compose the 3D encoder  $\epsilon^{3d}$  in the 3D module.

**Text Encoder.** We take the text encoder of a large-scale vision-language model CLIP (Radford et al. 2021) (other VLMs are also practicable and we choose CLIP in this paper) as the text encoder  $\epsilon^{text}$  to extract query embedding  $F^Q \in \mathbb{R}^{1 \times d}$  of  $Q$ . Meanwhile, each category label in the full category list of the 3D-VG dataset is also encoded by  $\epsilon^{text}$ , and represented by the category embeddings  $F^C \in \mathbb{R}^{K \times d}$ , where  $K$  denotes the category numbers. Dur-

ing training, we freeze the  $\epsilon^{text}$  and directly load the CLIP pretrained parameters.

**2D Encoder.** For each 3D proposal candidate, we project its point clouds onto  $L$  sampled frames (Dai et al. 2017) in the original video through geometric camera calibration, and get the corresponded 2D image regions. Actually, we find that each 3D proposal may have multiple correspondences in different frames in the video and therefore refer to multiple 2D image regions. Here, we only choose the 2D image region which contains the most 3D projected points from the point cloud, to pair with the 3D proposal candidate. We leverage the image encoder of CLIP  $\epsilon^{2d}$  to extract the 2D semantic embeddings of these 2D image regions, which are denoted as  $F^{2D} = \{F_1^{2D}, \dots, F_M^{2D}\}$ . Similarly, we also freeze  $\epsilon^{2d}$  and directly load the CLIP pretrained parameters.

**Cross-Modal Contrastive Learning.** Since large-scale vision language models such as CLIP has established a high level of semantic alignment between 2D image embeddings and text embeddings, and we also conveniently get the 2D correspondence of each 3D point cloud proposal, we can naturally take the 2D embedding as a bridge to implicitly align the 3D embedding and text embedding with a contrastive learning process. Specifically, we follow the typical

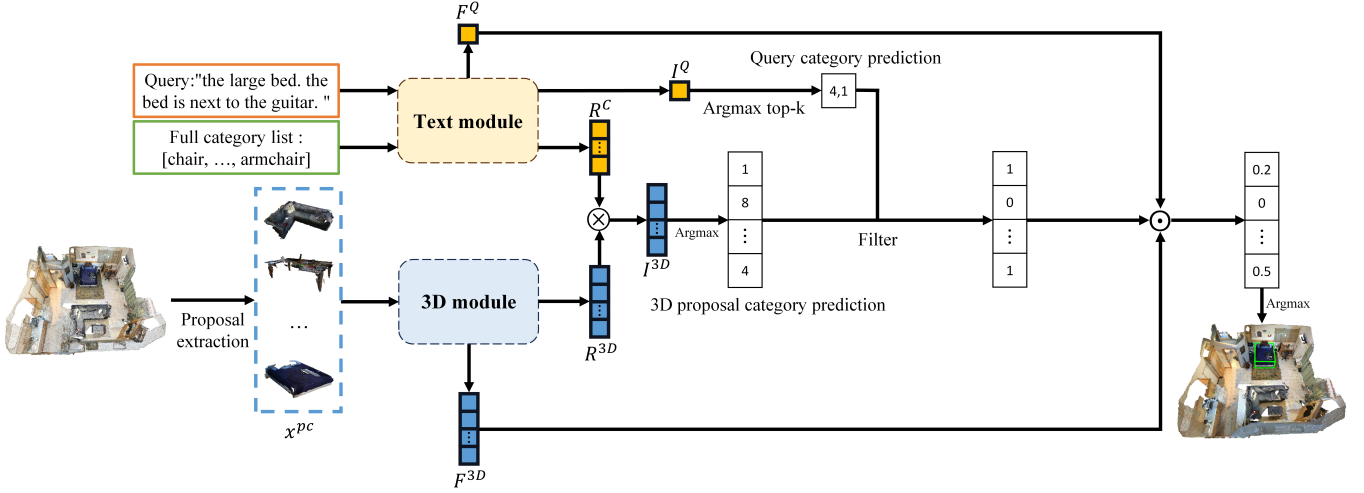


Figure 3: The inference procedure of our proposed 3D-VLA. Here, we only keep the text and 3D modules and does not need the 2D module. 3D proposal candidates and their embeddings ( $F^{3D}$  and  $R^{3D}$ ) are obtained from the 3D module. Text query embedding  $F^Q$  and category label embedding  $R^C$  are obtained from the text module. We perform matrix multiplication on  $R^{3D}$  and  $R^C$ , and get the 3D proposal category prediction, and then utilize the query category prediction to filter out those proposals with different classifying results with it. For the reserved 3D proposals, we rank them by the inner product similarity between their 3D embeddings  $F^{3D}$  and the text query embedding  $F^Q$ , and choose the top-1 proposal as the final predicted target proposal corresponding to the text query.

contrastive loss (Khosla et al. 2020) by pulling embeddings of the paired 3D proposal and 2D region closer, and pushing apart the unpaired one. The concrete definition is as follows:

$$\mathcal{L}_e = -\frac{1}{|M|} \sum_{i \in M} \left( \log \frac{\exp((F_i^{2D} \cdot F_i^{3D})/\tau)}{\sum_{j \in M} \exp((F_i^{2D} \cdot F_j^{3D})/\tau)} + \log \frac{\exp((F_i^{2D} \cdot F_i^{3D})/\tau)}{\sum_{j \in M} \exp((F_j^{2D} \cdot F_i^{3D})/\tau)} \right). \quad (1)$$

where  $\tau$  is the temperature hyper-parameter. By optimizing the  $\mathcal{L}_e$  loss above, we could make the learned 3D encoder  $\varepsilon^{3d}$  generate 3D proposal embedding align with its 2D image embedding, thus make it comparable to text embeddings of queries.

**Multi-Modal Adaption Through Task-Aware Classification.** As we known, the large-scale pretrained data of CLIP are free and general, and they do not have specialized knowledge to point cloud scenes. Therefore, only relying on the VLMs to build the 3D-text correlation will make the 3D-VG process not reliable. To mitigate this issue, we propose to introduce auxiliary 3D-VG task-aware classification to adapt the learned multi-modal embeddings better aligned in the point cloud scene.

Specifically, as shown in Fig. 2, we first add an adapter each to the text, 2D and 3D modules. All these adapters are with the same structure (two fully-connected layers with ReLU activate function), and residual connections are employed to keep both the source and adapted semantics:

$$R^* = \alpha \cdot A^* + (1 - \alpha) \cdot F^*, \quad (2)$$

where  $\alpha$  is the ratio of residual connections. Meanwhile, to further ensure a cohesive connection between the 2D and

3D embeddings after the adaption procedure, we also introduce a contrastive loss  $\mathcal{L}_a$  to the adapted 2D and 3D embeddings  $A_{2D}$  and  $A_{3D}$ . Here,  $\mathcal{L}_a$  fully follows  $\mathcal{L}_e$  above and we omit its definition in this section.

Furthermore, to bring in the 3D-VG task-aware semantic knowledge to the overall model, we introduce three classification tasks based on the residual embeddings  $R^Q$ ,  $R^{2D}$ , and  $R^{3D}$ . We first add a text classifier on the residual query embedding  $R^Q$  to predict the distribution on the category labels of the 3D-VG dataset, supervised by a cross-entropy loss  $\mathcal{L}_{cls}^q$ , which we denote as query classification loss. For the 2D and 3D classification, we adopt a task-aware classification strategy. As we mentioned before, all the category labels are encoded by the text encoder  $\varepsilon^{text}$ , here we also input all the category embeddings to the adapter in the text module, and thus obtain the residual category embeddings  $R^C$ . We perform matrix multiplication on  $R^C \in \mathbb{R}^{K \times d}$  and the 2D residual embeddings  $R^{2D} \in \mathbb{R}^{M \times d}$ , and thus get the 2D classification logits  $I^{2D} \in \mathbb{R}^{M \times K}$ . Softmax layer is applied on  $I^{2D}$  and a 2D classification cross-entropy loss  $\mathcal{L}_{cls}^{2d}$  is introduced to supervise the above 2D image classification procedure. Symmetrically, we can also compute the 3D classification loss  $\mathcal{L}_{cls}^{3d}$ .

Just by introducing the above coarse-grained classification signals while without the need for fine-grained box annotations, we can make the learned adapted embeddings have better semantic awareness of the point clouds of indoor scenes, thus assisting the 3D-VG process.

**Overall Loss Functions.** Combining the above contrastive losses  $\mathcal{L}_e$  and  $\mathcal{L}_a$ , as well as the query, 2D and 3D classification losses  $\mathcal{L}_{cls}^q$ ,  $\mathcal{L}_{cls}^{2d}$  and  $\mathcal{L}_{cls}^{3d}$ , our overall model is



Supervision	Method	Pub.	Input	Unique		Multiple		Overall	
				Acc@0.25	Acc@0.50	Acc@0.25	Acc@0.50	Acc@0.25	Acc@0.50
Fully Supervised	ReferIt3D	ECCV20	3D	53.75%	37.47%	21.03%	12.83%	26.44%	16.90%
	ScanRefer	ECCV20	3D	67.64%	46.19%	32.06%	21.26%	38.97%	26.10%
			3D+2D	76.33%	53.51%	32.73%	21.11%	41.19%	27.40%
	TGNN	AAAI21	3D	68.61%	56.80%	29.84%	23.18%	37.37%	29.70%
	InstanceRefer	ICCV21	3D	77.45%	66.83%	31.27%	24.77%	40.23%	32.93%
	SAT	ICCV21	3D+2D	73.21%	50.83%	37.64%	25.16%	44.54%	30.14%
	3D-SPS	CVPR22	3D+2D	84.12%	66.72%	40.32%	29.82%	48.82%	36.98%
Weakly Supervised	EDA	CVPR23	3D	85.76%	68.57%	49.13%	37.64%	54.59%	42.26%
	Ours	-	3D+2D	72.95%	62.17%	22.77%	17.94%	32.51%	26.53%

Table 1: Performance comparison on the ScanRefer dataset.

Supervision	Method	Pub.	Overall	Easy	Hard	View-dep.	View-indep.
Nr3d							
Fully Supervised	ReferIt3D	ECCV20	35.6%±0.7%	43.6%±0.8%	27.9%±0.7%	32.5%±0.7%	37.1%±0.8%
	TGNN	AAAI21	37.3%±0.3%	44.2%±0.4%	30.6%±0.2%	35.8%±0.2%	38.0%±0.3%
	InstanceRefer	ICCV21	38.8%±0.4%	46.0%±0.5%	31.8%±0.4%	34.5%±0.6%	41.9%±0.4%
	SAT	ICCV21	49.2%±0.3%	56.3%±0.5%	42.4%±0.4%	46.9%±0.3%	50.4%±0.3%
	LanguageRefer	CoRL22	43.9%	51.0%	36.6%	41.7%	45.0%
	3D-SPS	CVPR22	51.5%±0.2%	58.1%±0.3%	45.1%±0.4%	48.0%±0.2%	53.2%±0.3%
	EDA	CVPR23	52.1%	-	-	-	-
Weakly Supervised	Ours	-	32.1%±0.2%	38.6%±0.2%	25.8%±0.3%	28.8%±0.3%	33.7%±0.4%
Sr3d							
Fully Supervised	ReferIt3D	ECCV20	40.8%±0.2%	44.7%±0.1%	31.5%±0.4%	39.2%±1.0%	40.8%±0.1%
	TGNN	AAAI21	45.0%±0.2%	48.5%±0.2%	36.9%±0.5%	45.8%±1.1%	45.0%±0.2%
	InstanceRefer	ICCV21	48.0%±0.3%	51.1%±0.2%	40.5%±0.3%	45.4%±0.9%	48.1%±0.3%
	SAT	ICCV21	57.9%	61.2%	50.0%	49.2%	58.3%
	LanguageRefer	CoRL22	56.0%	58.9%	49.3%	49.2%	56.3%
	3D-SPS	CVPR22	62.6%±0.2%	56.2%±0.6%	65.4%±0.1%	49.2%±0.5%	63.2%±0.2%
	EDA	CVPR23	68.1%	-	-	-	-
Weakly Supervised	Ours	-	34.5%±0.2%	37.7%±0.2%	27.0%±0.4%	35.3%±0.5%	34.5%±0.2%

Table 2: Performance comparison on the ReferIt3D (Nr3D and Sr3D) dataset.

optimized by:

$$\mathcal{L} = \beta * (\mathcal{L}_e + \mathcal{L}_a) + \mathcal{L}_{cls}^{2d} + \mathcal{L}_{cls}^{3d} + \mathcal{L}_{cls}^q, \quad (3)$$

where  $\beta$  controls the ratio of each loss term. We set  $\beta = 0.5$  by default.

### 3D-VLA Inference with Category-Oriented Proposal Filtering

In the inference stage, as shown in Fig. 3, we only retain the 3D and text modules and does not need the 2D module’s involvement.

Firstly, we take the 3D proposal embeddings  $F^{3D}$  and its residual embeddings  $R^{3D}$  from the 3D module, as well as the text query embedding  $F^Q$  and the category residual embeddings  $R^C$  from the text module.  $I^Q$  is also computed to get the query classification result on the 3D-VG categories. By performing matrix multiplication on  $R^{3D}$  and  $R^C$ , we can get the category prediction of each 3D proposal. In order to make the category corresponding to the target proposal more consistent with the category corresponding to the query, we propose a category-oriented proposal filtering strategy by only keeping the 3D proposals that have the same category prediction with the top- $k$  categories of the text query. For instance, as shown in Fig. 3, if the top-2 category predictions of the query are “bed” (id: 4) and “sofa” (id:

1), we only keep 3D proposals whose category prediction belonging to these two categories and create a mask, 1 for the reserved proposal and 0 for the filtered one. Finally, for the reserved proposals, we rank them by their inner product similarity between their 3D embeddings  $F^{3D}$  and the query embedding  $F^Q$ , and choose the proposal with the highest similarity score as the predicted target proposal.

Also noted that, if the category predictions of all 3D proposals do not match with that of the query, we keep all the proposals and do not perform the filtering strategy.

## Experiments

In this section, we first present our experimental settings include datasets, evaluation metrics and our implementation details. Then, we will demonstrate our 3D-VLA results and discuss the effectiveness of each our model component.

### Experiment Settings

**Dataset.** We evaluate our 3D-VLA on two public and widely-used datasets **ScanRefer** (Chen, Chang, and Nießner 2020) and **ReferIt3D** (Achlioptas et al. 2020).

The ScanRefer dataset is derived from indoor 3D scene dataset ScanNet (Dai et al. 2017). It is divided into two distinct parts: “Unique” and “Multiple”, which indicate that whether the scene contains more than two distractors.

	$\mathcal{L}_e$	$\mathcal{L}_{cls}$	Filter	Adapter	$\mathcal{L}_a$	Overall	Easy	Hard	View-dep.	View-indep.
(a)	✓					17.5%±0.3%	20.9%±0.4%	14.2%±0.3%	13.5%±0.4%	19.4%±0.4%
(b)	✓	✓				21.8%±0.2%	26.8%±0.3%	17.0%±0.4%	16.8%±0.4%	24.3%±0.3%
(c)	✓	✓	✓			29.7%±0.4%	36.7%±0.4%	23.0%±0.4%	28.3%±0.3%	30.4%±0.4%
(d)	✓	✓	✓	✓		30.8%±0.3%	38.6%±0.6%	23.4%±0.2%	28.6%±0.4%	32.0%±0.3%
(e)	✓	✓	✓	✓	✓	32.1%±0.2%	38.6%±0.2%	25.8%±0.3%	28.8%±0.3%	33.7%±0.4%

Table 3: Ablation studies of the 3D-VLA components on Nr3D.

Top-k	Overall	Easy	Hard	View-dep.	View-indep.
1	31.4%±0.2%	38.9%±0.4%	24.2%±0.5%	28.2%±0.4%	33.0%±0.2%
2	31.8%±0.2%	38.5%±0.4%	25.3%±0.5%	29.7%±0.4%	32.8%±0.4%
3	32.1%±0.2%	38.6%±0.2%	25.8%±0.3%	28.8%±0.3%	33.7%±0.4%
4	31.7%±0.3%	38.9%±0.5%	24.8%±0.1%	28.5%±0.2%	33.3%±0.4%

Table 4: 3D-VLA performance with different  $k$  in the category-oriented proposal filtering strategy on Nr3D.

The ReferIt3D dataset is also proposed based on the ScanNet dataset. It consists of two subsets: Sr3D and Nr3D. Two distinct data splits are employed in Sr3D and Nr3D. The “Easy” and “Hard” splits are divided based on the number of distractors in the scene, and the “View-dep.” and “View-indep.” splits are divided based on whether the referring expression is dependent on the speaker’s view.

With regard to the ReferIt3D dataset, it has provided 3D proposals as well as the category labels of them in the indoor point cloud scene. Therefore, we can directly use the provided proposals as the 3D proposal candidates, and leverage the provided category labels to provide the coarse-grained supervision signals to the model. However, for the ScanRefer dataset, it does not provide the above two terms. Therefore, we employ the pretrained PointGroup (Jiang et al. 2020) as the detector to extract the proposals as well as their category labels in advance, and then utilize the pre-extracted information to help the model training.

**Evaluation Metric.** For the ScanRefer dataset, we follow InstanceRefer (Yuan et al. 2021), and take  $\text{Acc}@m\text{IoU}$  as the evaluation metric, where  $m$  takes on values from the set  $\{0.25, 0.5\}$ .

Since ReferIt3D dataset has provided several 3D proposals as the candidates for visual grounding, it converts the 3D-VG task into a classification problem, *i.e.*, whether the selected proposal among the  $M$  candidates is the groundtruth proposal. Models are thus evaluated by accuracy, which measures the percentage of the correct selected samples.

**Implementations Details.** 3D-VLA is implemented by PyTorch (Paszke et al. 2019). Model optimization is conducted using Adam optimizer (Kingma and Ba 2015) with batch size of 32. We set an initial learning rate of 0.0005 for the model, and the learning rate of the transformer layer is further adjusted by multiplying it with 0.1. We reduce the learning rate by a multiplicative factor of 0.65 at epochs 20, 30, 40, and 50. The CLIP embedding dimension  $d$  is 512, and the hidden dimension in our adapters is also set as 512. Besides, we set  $k = 3$  as default in category-oriented proposal filtering module.

### 3D Visual Grounding Results

**ScanRefer.** For the ScanRefer dataset, we present the  $\text{Acc}@m\text{IoU}$  performances in Table. 1. We also indicate the used input modalities of each method (purely 3D or 3D+2D). It can be observed that, although our weakly-supervised 3D-VLA has a certain gap with the leading SOTAs, we are also supervised to find that our method even outperforms some fully supervised methods. Specifically, our 3D-VLA greatly surpasses the ReferIt3D baseline (Achlioptas et al. 2020) in all subsets. Furthermore, in the “Unique” subset, our model outperforms the ScanRefer baseline with 3D input (Chen, Chang, and Nießner 2020) and TGNN (Huang et al. 2021) by 5.31% and 4.34% on  $\text{Acc}@0.25$ , and 15.98% and 5.37% on  $\text{Acc}@0.50$ , respectively. Although ScanRefer with 3D+2D input performs better at  $\text{Acc}@0.25$ , 3D-VLA outperforms it by a large margin on the more challenging  $\text{Acc}@0.50$ . Meanwhile, our 3D-VLA also has a 11.34% improvement on  $\text{Acc}@0.50$  over SAT (Yang et al. 2021), from 50.83% to 62.17% in the “Unique” subset.

**ReferIt3D.** In Table. 2, we present the performance results of 3D-VLA on the ReferIt3D dataset, in comparison to the supervised models. Although our 3D-VLA does not completely outperform the supervised models across all the subsets, but the performance is still comparable. Such results demonstrate the effectiveness and potential of our weakly supervised training diagram, which does not leverage any 3D box annotations or explicit 3D-Text correspondence supervision.

### Ablation Studies

**Effectiveness of Each Components.** In order to explore the effectiveness of the each component in our 3D-VLA, we conduct comprehensive ablation studies on the Nr3D dataset (Achlioptas et al. 2020), as shown in Table. 3. The ablation model (a) only retains and text, 2D and 3D encoders while drops the adapters and does not use the filtering strategy. It is merely trained with the contrastive loss  $\mathcal{L}_e$ . The model (b), also does not involve adapters, but directly applies the classification losses on  $F^Q$ ,  $F^{2D}$ , and  $F^{3D}$ . Compared (b) to (a), we can find that introducing task-aware classification signals to guide model is beneficial to increase

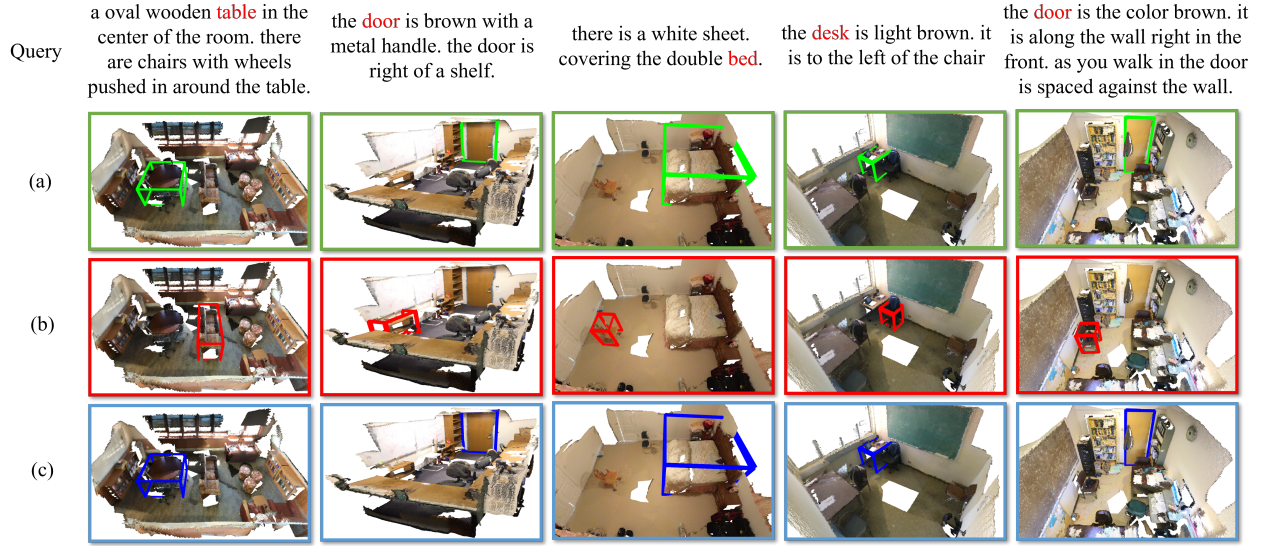


Figure 4: The qualitative results of our 3D-VLA. We use green/red/blue colors to represent the ground truth/incorrect predictions/correct predictions. (a) shows the ground truth, (b) and (c) show our model predictions w/o and w/ category-oriented proposal filtering strategy, respectively.

the 3D-VG accuracy. When we add the category-oriented proposal filtering in (c), the overall performance is greatly improved from 21.8% to 29.7%. This observation proves the effectiveness of the category-oriented proposal filtering strategy, which can filter out some confused 3D proposals with different category labels to the queries, and thus get clearer and better quality 3D proposal candidates for visual grounding. Furthermore, by introducing adapters in model (d), the performance of 3D-VLA also gets promotion. This proves that our multi-modal adaptation design can help to get a better, indoor point cloud specific embedding space to align 3D point clouds and text queries. Finally, when introducing contrastive loss  $\mathcal{L}_a$  on the adapted embeddings, the overall model performance increases from 30.8% to 32.1%, and the improvements mainly come from the “Hard” subset and “View-indep.” subset. Such results show that keeping cohesive connection between the adapted embedding is beneficial for the model to identify some objects that are difficult to distinguish.

**Investigating the Influence of Top- $k$  Query Category Predictions in Proposal Filtering.** We investigate the influence of using different top- $k$  query category predictions in our category-oriented proposal filtering strategy. The experiments are conducted on the Nr3D dataset, and the results are shown in Table. 4. We set  $k$  in four different values, *i.e.*,  $k \in \{1, 2, 3, 4\}$ . It can be observed that keeping more query category predictions brings higher accuracy, which shows that keeping more possible categories from the query could provide more semantic information to filter invalid 3D proposals, and is helpful to 3D-VG. We take  $k = 3$  as the default setting since a value of  $k$  that is too large might introduce an excess of interference candidates, leading to a negative impact on the network’s performance.

**Qualitative Results.** The qualitative results of 3D-VLA are shown in Fig. 4. Compare the predictions from the row (b) to the row (c), we can find that our category-oriented proposal filtering can filter out invalid 3D proposals that have error category predictions, and thus avoid these proposals to interfere the ranking procedure of the reserved proposals.

## Conclusion

In this paper, we propose to tackle the weakly supervised 3D visual grounding from a novel perspective towards Visual Linguistic Alignment, in an effort to address the shortage of fine-grained box annotations. Specifically, our 3D-VLA leverages the superior ability of current advanced VLMs to align the semantics among texts and 2D images, as well as the naturally existing correspondences between 2D images and 3D point clouds, such that implicitly constructing correspondences between texts and 3D point clouds. During 3D-VLA inference, we exploit the learned text-3D correspondence to help ground the text queries to the referred 3D objects without regarding to 2D images. Through the designed scheme, a significant breakthrough is achieved than previous works, and the advantage of our 3D-VLA are also analyzed in detail. We believe these analyses can provide valuable insights to facilitate the future research of weakly supervised 3D visual grounding.

## References

Achlioptas, P.; Abdelreheem, A.; Xia, F.; Elhoseiny, M.; and Guibas, L. 2020. Referit3d: Neural listeners for fine-grained 3d object identification in real-world scenes. In *Computer Vision–ECCV 2020: 16th European Conference, Glasgow, UK, August 23–28, 2020, Proceedings, Part I* 16, 422–440. Springer.

- Bakr, E.; Alsaedy, Y.; and Elhoseiny, M. 2022. Look around and refer: 2d synthetic semantics knowledge distillation for 3d visual grounding. *Advances in Neural Information Processing Systems*, 35: 37146–37158.
- Bao, H.; Wang, W.; Dong, L.; Liu, Q.; Mohammed, O. K.; Aggarwal, K.; Som, S.; Piao, S.; and Wei, F. 2022. Vlmo: Unified vision-language pre-training with mixture-of-modality-experts. *Advances in Neural Information Processing Systems*, 35: 32897–32912.
- Chen, D. Z.; Chang, A. X.; and Nießner, M. 2020. Scanrefer: 3d object localization in rgb-d scans using natural language. In *European conference on computer vision*, 202–221. Springer.
- Chen, D. Z.; Wu, Q.; Nießner, M.; and Chang, A. X. 2022a. D 3 Net: A Unified Speaker-Listener Architecture for 3D Dense Captioning and Visual Grounding. In *European Conference on Computer Vision*, 487–505. Springer.
- Chen, J.; Luo, W.; Wei, X.; Ma, L.; and Zhang, W. 2022b. Ham: Hierarchical attention model with high performance for 3d visual grounding. *arXiv preprint arXiv:2210.12513*.
- Chen, K.; Gao, J.; and Nevatia, R. 2018. Knowledge aided consistency for weakly supervised phrase grounding. In *Proceedings of the IEEE Conference on Computer Vision and Pattern Recognition*, 4042–4050.
- Dai, A.; Chang, A. X.; Savva, M.; Halber, M.; Funkhouser, T.; and Nießner, M. 2017. Scannet: Richly-annotated 3d reconstructions of indoor scenes. In *Proceedings of the IEEE conference on computer vision and pattern recognition*, 5828–5839.
- Datta, S.; Sikka, K.; Roy, A.; Ahuja, K.; Parikh, D.; and Divakaran, A. 2019. Align2ground: Weakly supervised phrase grounding guided by image-caption alignment. In *Proceedings of the IEEE/CVF international conference on computer vision*, 2601–2610.
- Dou, Z.-Y.; and Peng, N. 2021. Improving pre-trained vision-and-language embeddings for phrase grounding. In *Proceedings of the 2021 Conference on Empirical Methods in Natural Language Processing*, 6362–6371.
- Feng, M.; Li, Z.; Li, Q.; Zhang, L.; Zhang, X.; Zhu, G.; Zhang, H.; Wang, Y.; and Mian, A. 2021. Free-form description guided 3d visual graph network for object grounding in point cloud. In *Proceedings of the IEEE/CVF International Conference on Computer Vision*, 3722–3731.
- Feng, Q.; Ablavsky, V.; and Sclaroff, S. 2021. Cityflow-nl: Tracking and retrieval of vehicles at city scale by natural language descriptions. *arXiv preprint arXiv:2101.04741*.
- Gao, P.; Geng, S.; Zhang, R.; Ma, T.; Fang, R.; Zhang, Y.; Li, H.; and Qiao, Y. 2021. Clip-adapter: Better vision-language models with feature adapters. *arXiv preprint arXiv:2110.04544*.
- Gupta, T.; Vahdat, A.; Chechik, G.; Yang, X.; Kautz, J.; and Hoiem, D. 2020. Contrastive learning for weakly supervised phrase grounding. In *European Conference on Computer Vision*, 752–768. Springer.
- He, D.; Zhao, Y.; Luo, J.; Hui, T.; Huang, S.; Zhang, A.; and Liu, S. 2021. Transrefer3d: Entity-and-relation aware transformer for fine-grained 3d visual grounding. In *Proceedings of the 29th ACM International Conference on Multimedia*, 2344–2352.
- Huang, P.-H.; Lee, H.-H.; Chen, H.-T.; and Liu, T.-L. 2021. Text-guided graph neural networks for referring 3d instance segmentation. In *Proceedings of the AAAI Conference on Artificial Intelligence*, volume 35, 1610–1618.
- Huang, S.; Chen, Y.; Jia, J.; and Wang, L. 2022. Multi-view transformer for 3d visual grounding. In *Proceedings of the IEEE/CVF Conference on Computer Vision and Pattern Recognition*, 15524–15533.
- Jain, A.; Gkanatsios, N.; Mediratta, I.; and Fragkiadaki, K. 2022. Bottom up top down detection transformers for language grounding in images and point clouds. In *European Conference on Computer Vision*, 417–433. Springer.
- Jia, C.; Yang, Y.; Xia, Y.; Chen, Y.-T.; Parekh, Z.; Pham, H.; Le, Q.; Sung, Y.-H.; Li, Z.; and Duerig, T. 2021. Scaling up visual and vision-language representation learning with noisy text supervision. In *International conference on machine learning*, 4904–4916. PMLR.
- Jiang, L.; Zhao, H.; Shi, S.; Liu, S.; Fu, C.-W.; and Jia, J. 2020. Pointgroup: Dual-set point grouping for 3d instance segmentation. In *Proceedings of the IEEE/CVF conference on computer vision and pattern recognition*, 4867–4876.
- Khosla, P.; Teterwak, P.; Wang, C.; Sarna, A.; Tian, Y.; Isola, P.; Maschinot, A.; Liu, C.; and Krishnan, D. 2020. Supervised contrastive learning. *Advances in neural information processing systems*, 33: 18661–18673.
- Kim, W.; Son, B.; and Kim, I. 2021. Vilt: Vision-and-language transformer without convolution or region supervision. In *International Conference on Machine Learning*, 5583–5594. PMLR.
- Kingma, D. P.; and Ba, J. 2015. Adam: A method for stochastic optimization.
- Li, J.; Jie, Z.; Wang, X.; Wei, X.; and Ma, L. 2022a. Expansion and shrinkage of localization for weakly-supervised semantic segmentation. *Advances in Neural Information Processing Systems*, 35: 16037–16051.
- Li, J.; Jie, Z.; Wang, X.; Zhou, Y.; Ma, L.; and Jiang, J. 2023. Weakly supervised semantic segmentation via self-supervised destruction learning. *Neurocomputing*, 561: 126821.
- Li, J.; Jie, Z.; Wang, X.; Zhou, Y.; Wei, X.; and Ma, L. 2022b. Weakly supervised semantic segmentation via progressive patch learning. *IEEE Transactions on multimedia*.
- Liu, X.; Li, L.; Wang, S.; Zha, Z.-J.; Meng, D.; and Huang, Q. 2019. Adaptive reconstruction network for weakly supervised referring expression grounding. In *Proceedings of the IEEE/CVF International Conference on Computer Vision*, 2611–2620.
- Liu, Y.; Wan, B.; Ma, L.; and He, X. 2021. Relation-aware instance refinement for weakly supervised visual grounding. In *Proceedings of the IEEE/CVF conference on computer vision and pattern recognition*, 5612–5621.
- Luo, J.; Fu, J.; Kong, X.; Gao, C.; Ren, H.; Shen, H.; Xia, H.; and Liu, S. 2022. 3d-sps: Single-stage 3d visual grounding via referred point progressive selection. In *Proceedings of*

- the *IEEE/CVF Conference on Computer Vision and Pattern Recognition*, 16454–16463.
- Mittal, V. 2020. Attngrounder: Talking to cars with attention. In *Computer Vision–ECCV 2020 Workshops: Glasgow, UK, August 23–28, 2020, Proceedings, Part II* 16, 62–73. Springer.
- Paszke, A.; Gross, S.; Massa, F.; Lerer, A.; Bradbury, J.; Chanan, G.; Killeen, T.; Lin, Z.; Gimelshein, N.; Antiga, L.; et al. 2019. Pytorch: An imperative style, high-performance deep learning library. *Advances in neural information processing systems*, 32.
- Qi, C. R.; Litany, O.; He, K.; and Guibas, L. J. 2019. Deep hough voting for 3d object detection in point clouds. In *proceedings of the IEEE/CVF International Conference on Computer Vision*, 9277–9286.
- Qi, C. R.; Yi, L.; Su, H.; and Guibas, L. J. 2017. Pointnet++: Deep hierarchical feature learning on point sets in a metric space. *Advances in neural information processing systems*, 30.
- Qu, T.; Tuytelaars, T.; and Moens, M.-F. 2023. Weakly supervised face naming with symmetry-enhanced contrastive loss. In *Proceedings of the IEEE/CVF Winter Conference on Applications of Computer Vision*, 3505–3514.
- Radford, A.; Kim, J. W.; Hallacy, C.; Ramesh, A.; Goh, G.; Agarwal, S.; Sastry, G.; Askell, A.; Mishkin, P.; Clark, J.; et al. 2021. Learning transferable visual models from natural language supervision. In *International conference on machine learning*, 8748–8763. PMLR.
- Roh, J.; Desingh, K.; Farhadi, A.; and Fox, D. 2022. Language-refer: Spatial-language model for 3d visual grounding. In *Conference on Robot Learning*, 1046–1056. PMLR.
- Rohrbach, A.; Rohrbach, M.; Hu, R.; Darrell, T.; and Schiele, B. 2016. Grounding of textual phrases in images by reconstruction. In *Computer Vision–ECCV 2016: 14th European Conference, Amsterdam, The Netherlands, October 11–14, 2016, Proceedings, Part I* 14, 817–834. Springer.
- Salvador, A.; Giró-i Nieto, X.; Marqués, F.; and Satoh, S. 2016. Faster r-cnn features for instance search. In *Proceedings of the IEEE conference on computer vision and pattern recognition workshops*, 9–16.
- Vaswani, A.; Shazeer, N.; Parmar, N.; Uszkoreit, J.; Jones, L.; Gomez, A. N.; Kaiser, Ł.; and Polosukhin, I. 2017. Attention is all you need. *Advances in neural information processing systems*, 30.
- Wang, L.; Li, Y.; Huang, J.; and Lazebnik, S. 2018. Learning two-branch neural networks for image-text matching tasks. *IEEE Transactions on Pattern Analysis and Machine Intelligence*, 41(2): 394–407.
- Wang, Q.; Tan, H.; Shen, S.; Mahoney, M. W.; and Yao, Z. 2020. Maf: Multimodal alignment framework for weakly-supervised phrase grounding. 2030–2038.
- Wu, Y.; Cheng, X.; Zhang, R.; Cheng, Z.; and Zhang, J. 2023. EDA: Explicit Text-Decoupling and Dense Alignment for 3D Visual Grounding. In *Proceedings of the IEEE/CVF Conference on Computer Vision and Pattern Recognition*, 19231–19242.
- Yang, S.; Li, G.; and Yu, Y. 2019. Cross-modal relationship inference for grounding referring expressions. In *Proceedings of the IEEE/CVF conference on computer vision and pattern recognition*, 4145–4154.
- Yang, Z.; Gong, B.; Wang, L.; Huang, W.; Yu, D.; and Luo, J. 2019. A fast and accurate one-stage approach to visual grounding. In *Proceedings of the IEEE/CVF International Conference on Computer Vision*, 4683–4693.
- Yang, Z.; Zhang, S.; Wang, L.; and Luo, J. 2021. Sat: 2d semantics assisted training for 3d visual grounding. In *Proceedings of the IEEE/CVF International Conference on Computer Vision*, 1856–1866.
- Yuan, Z.; Yan, X.; Liao, Y.; Zhang, R.; Wang, S.; Li, Z.; and Cui, S. 2021. Instancerefer: Cooperative holistic understanding for visual grounding on point clouds through instance multi-level contextual referring. In *Proceedings of the IEEE/CVF International Conference on Computer Vision*, 1791–1800.
- Zhang, H.; Niu, Y.; and Chang, S.-F. 2018. Grounding referring expressions in images by variational context. In *Proceedings of the IEEE Conference on Computer Vision and Pattern Recognition*, 4158–4166.
- Zhao, L.; Cai, D.; Sheng, L.; and Xu, D. 2021. 3DVG-Transformer: Relation modeling for visual grounding on point clouds. In *Proceedings of the IEEE/CVF International Conference on Computer Vision*, 2928–2937.
- Zhou, K.; Yang, J.; Loy, C. C.; and Liu, Z. 2022a. Conditional prompt learning for vision-language models. In *Proceedings of the IEEE/CVF Conference on Computer Vision and Pattern Recognition*, 16816–16825.
- Zhou, K.; Yang, J.; Loy, C. C.; and Liu, Z. 2022b. Learning to prompt for vision-language models. *International Journal of Computer Vision*, 130(9): 2337–2348.